DRAFT

Proceedings of the 9th International Pipeline Conference
IPC2012
September 24-28, 2012, Calgary, Alberta, Canada

IPC2012-90736

INFLUENCE OF GIRTH WELD FLAW AND PIPE PARAMETERS ON THE CRITICAL LONGITUDINAL STRAIN OF STEEL PIPES

Celal Cakiroglu
Department of Civil and Environmental Engineering, University of Alberta
Edmonton, Alberta, Canada

Kajsa Duke
Department of Mechanical Engineering, University of Alberta
Edmonton, Alberta, Canada

Marwan El-Rich
Department of Civil and Environmental Engineering, University of Alberta
Edmonton, Alberta, Canada

Samer Adeeb
Department of Civil and Environmental Engineering, University of Alberta
Edmonton, Alberta, Canada

J. J. Roger Cheng
Department of Civil and Environmental Engineering, University of Alberta
Edmonton, Alberta, Canada

Millan Sen
Enbridge Pipelines Inc.
Edmonton, Alberta, Canada

ABSTRACT
The design of steel pipelines against longitudinal loading induced by soil movement and temperature requires an understanding of the strain demand induced by the environment in comparison with the strain resistance of the pipes. Girth weld flaws have been identified as the potential location of failure under longitudinal tensile strains due to being the least ductile. Strain based design for the prediction of the longitudinal tensile strain capacity of steel pipes have been extensively studied by Wang, et al and included in the Canadian standards association code of practice CSA Z662.11. The extensive track record of tests have culminated into two sets of equations for the critical strain in girth welded pipes with surface breaking and buried defects as functions of the different pipe and flaw parameters.

The CSA Z662.11 strain capacity equations were developed using wide plate tests with the obvious limitation of the inability to consider the effect of the internal pressure of the pipe. However, recent studies by Wang et al led to the development of a new set of equations that predict the tensile strain capacity for pipes with an internal pressure factor of 0.72.

This paper analyses the two critical strain equations in CSA Z662-11 to understand the effect of different girth weld flaw and pipe parameters on the expected behavior of pipes. Also the critical strain equations developed in [6] have been analysed and compared to the equations in CSA Z662-11. Using the equations in CSA Z662-11, a 3^4 and 3^6 full factorial experimental design was conducted for the planar surface-breaking defect and the planar buried defect respectively. For the case of surface breaking defects the

dependence of the tensile strain capacity (ε_t^{crit}) on apparent CTOD toughness (δ), ratio of defect height to pipe wall thickness (η), ratio of yield strength to tensile strength (λ) and the ratio of defect length to pipe wall thickness (ξ) has been studied. ε_t^{crit} has been evaluated at the maximum, minimum and intermediate values of each parameter according to the allowable ranges given in the code which resulted in the evaluation of ε_t^{crit} for 81 different combinations of the parameters. The average value of ε_t^{crit} at the maximum, minimum and middle value of each parameter has been calculated. The visualization of the results showed that η, δ and ξ have the most significant effect on ε_t^{crit} among the four parameters for the case of surface breaking defect.

Similarly for buried defects the dependence of ε_t^{crit} on δ, η, λ, ξ, and the pipe wall thickness (t) has been studied. The evaluation of ε_t^{crit} for all possible combinations of the maximum, intermediate and minimum values of the 6 parameters resulted in ε_t^{crit} values for 729 different combinations. The variation of the average ε_t^{crit} over the maximum, intermediate and minimum values of the parameters showed that δ, ψ, ξ and η are the parameters having the greatest effect on ε_t^{crit} for the case of a buried defect.

Further investigations could be carried out to determine suitable upper and lower bounds for the parameters for which no bounded range is defined in the CSA Z662-11 code.

INTRODUCTION

Steel pipelines are used for the efficient transportation of oil and natural gas from remote regions like sub-Arctic region of North America to the place of consumption. These pipelines are often subjected to excessive bending, tensile loading and high longitudinal strains due to temperature differences, internal pressure and unfavourable geotechnical conditions. The latter include slope instability, seismic activity or discontinuous permafrost which causes differential settlement of the pipeline due to the freezing and

Nomenclature

ε_t^{crit}	Tensile strain capacity
δ	Apparent crack-tip opening displacement (CTOD) toughness [mm]
η	Ratio of defect height to pipe wall thickness
λ	Ratio of yield strength to tensile strength (Y/T)
ξ	Ratio of defect length to pipe wall thickness
ψ	Ratio of defect depth to pipe wall thickness
a	Defect height for surface –breaking defect [mm]
$2a$	Defect height for buried defect [mm]
$2c$	Defect length [mm]
t	Pipe wall thickness [mm]
d_1	Defect depth [mm] (Figure 2)
f_p	Ratio of the applied hoop stress to the pipe yield strength (pressure factor)
σ_U^W	Weld metal ultimate tensile strength
σ_U	Base metal ultimate tensile strength
ϕ	Weld metal strength mismatch ratio (σ_U^W / σ_U)
h	Girth weld high-low misalignment [mm]
TSC_p	ε_t^{crit} of pipes with $t = 15.9$[mm] and $f_p = 0.72$
TSC_0	ε_t^{crit} of non-pressurized pipes

thawing cycle of the permafrost. In the presence of girth weld flaws, pressurized pipelines exhibit a reduction in their tensile strain capacity under tensile axial and bending loads. Extensive research has

been conducted by Wang, et al [1] , [2] , [3] , [4] , [5] to understand this reduction which culminated in equations for the prediction of the tensile strain capacity of steel pipes which have been included in the CSA Z662.11 code. Possible girth weld defects are classified by Wang et al as surface breaking defects and buried defects. Surface breaking defects are those that resemble a crack that is connected to the surface of the pipe, while buried defects are those that are not connected to the surface of the pipe. Surface breaking defects and buried defects are shown in Figure 1 and Figure 2 respectively. Although the buried defect type is considered to be less harmful compared to surface defects and often treated conservatively as surface breaking defects, according to Wang et al [1] it is demonstrated that this is not a right treatment. Therefore for each type of weld defect suitable equations are developed in order to predict ε_t^{crit} as a function of $\delta, \eta, \lambda, \xi$ for surface-breaking defects where η depends on defect height (a) and pipe wall thickness (t) and ξ depends on the defect length $(2c)$ and t and as a function of $\delta, \eta, \lambda, \xi, \psi$ for buried defects where ψ depends on the defect depth (d_1) and t. According to Z662-11, in the absence of any experimental data, ε_t^{crit} of the pipe material can be calculated based on the equations (1) and (3).

The original equations – which have also been adopted in CSA Z662.11 – have been developed based on wide plate tests which do not take the internal pressure of the pipe into consideration. This limitation has led to research towards the development of new sets of equations that are based on studies that include the internal pressure. Another set of tensile strain capacity equations has been proposed in [6] for a default pipe wall thickness of 15.9 mm and pressure factor (f_p) of 0.72 which denotes the ratio of applied hoop stress to pipe yield strength, in order to develop a new tensile strain design model which is an important part of the strain-based design of pipelines. These equations predict tensile strain capacities according to the type of welding and consider the effects of weld metal strength mismatch ratio (ϕ) and girth weld high-low misalignment (h) on the tensile strain capacity .

The development of the closed form equations for the critical strain capacity has finally enabled a rigorous methodological approach for the development of acceptance criteria for flaws in girth welds. However, a quick glance at equations (1) and (3) shows that these equations are highly nonlinear. In addition, it might not be possible using simple inspection to explain how sensitive the strain capacity of a pipeline is to the variation in the different variables. Furthermore, a new pipeline construction would require criteria for the inspection and identification of critical flaws; an indirect application of the developed equations. The main purpose of this paper is to fully understand the effect of the different pipe and girth weld flaw parameters on the expected tensile strain capacity of girth-welded steel pipelines and to analyze the sensitivity of the equations to the changes in the geometry and material properties. The methodological approach developed in this study can be adopted in a new pipeline construction project to create acceptance criteria for girth weld defects.

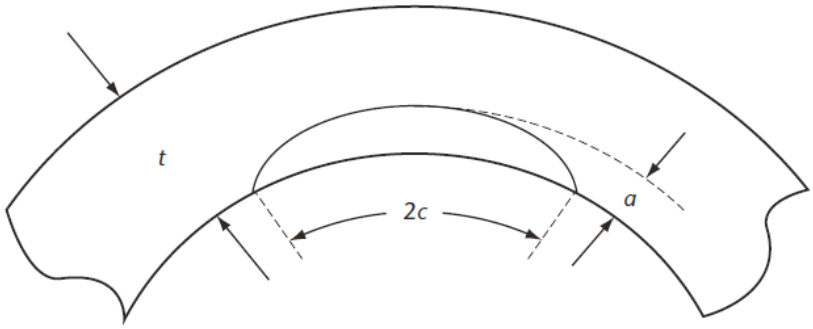

Figure 1: A planar surface-breaking defect in the pipe wall [8]

$$\varepsilon_t^{crit} = \delta^{2.36-1.58\lambda-0.101\xi\eta}(1 + 16.1\lambda^{-4.45})(-0.157 + 0.239\xi^{-0.241}\eta^{-0.315}) \quad (1)$$

$$\varepsilon_t^{crit} = \varepsilon_t^{crit}(\delta, \xi, \eta, \lambda) \quad (2)$$

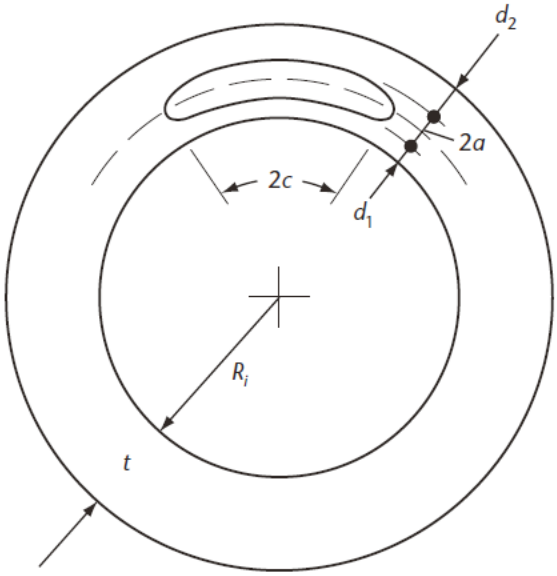

Figure 2: A planar buried defect in the pipe wall [8]

$$\varepsilon_t^{crit} = \delta^{(1.08-0.612\eta-0.0735\xi+0.364\psi)}\left(12.3 - 4.65\sqrt{t} + 0.495t\right)(11.8 - 10.6\lambda)$$
$$\left(-5.14 + \frac{0.992}{\psi} + 20.1\psi\right)\left(-3.63 + 11.0\sqrt{n} - 8.44\eta\right) \quad (3)$$
$$\left(-0.836 + 0.733\eta + 0.0483\xi + \frac{3.49 - 14.6\eta - 12.9\psi}{1 + \xi^{1.84}}\right)$$

$$\varepsilon_t^{crit} = \varepsilon_t^{crit}(\delta, \xi, \eta, \lambda, \psi, t) \quad (4)$$

ANALYSIS OF THE TENSILE STRAIN CAPACITY PREDICTION EQUATIONS

Surface breaking defects and buried defects are analysed using equations (1) and (3) respectively. In the analysis of surface breaking defects the prediction of Eq. (1) has been compared with the prediction of another tensile strain capacity equation developed in [6] and the comparison is visualized using surface plots in Figure 3 and Figure 4 . On these surface plots the variation of the ε_t^{crit} value with changing defect geometry for constant material properties has been visualized.

The variation of the ε_t^{crit} value predicted by Eq. (1) with changing material toughness and changing Y/T ratio for constant geometric parameters has been investigated separately using the curves in Figure 5. This analysis has been carried out for three different values of ξ and the results have been compared. The percent change in ε_t^{crit} has been plotted with respect to the percent change in apparent CTOD toughness and percent change in Y/T ratio for three different values of ξ.

In the next step of the analysis a 3^4 and 3^6 full factorial experimental design was conducted for the planar surface-breaking defect and the planar buried defect respectively based on the equations in the CSA code. This experimental design was adapted from the book of Montgomery, D [7] which gives information about factorial designs that can be used to investigate the effects of two or more factors where each effecting factor has different levels on a particular quantity for all possible combinations of the levels of the factors. The full factorial experimental designs made it possible to visualize the effect of each parameter on the tensile strain capacity by taking the average of ε_t^{crit} evaluated at the low, intermediate and high value of the range defined for each parameter by all possible combinations of the rest of the parameters and later generating 2 dimensional plots of these average values. The comparison of the 2 dimensional plots for each parameter gives an idea about the sensitivity of the equations (1) and (3) with respect to each parameter.

In order to apply the experimental design a special algorithm has been developed which traverses all possible values of the defect parameters and material properties in predefined ranges and evaluates the corresponding tensile strain capacities. In order to define the ranges of the parameters the values listed in the CSA Z662.11 code have been applied. These ranges are $0.7 \leq \lambda \leq 0.95$, $0.1 \leq \delta \leq 0.3$, $1 \leq \xi \leq 10$ and $\eta \leq 0.5$. Since the lower limit of η was not given it was set at 0.1 since for η values lower than 0.1 the crack size is negligible. Also impractically high values are predicted for ε_t^{crit} at values for η lower than 0.1. Also, since for the variable ψ no bounded range is defined in the code, an upper and lower bound in the same order of magnitude as η have been assumed which guarantees that the flaw is always buried within the pipe wall. For the pipe wall thickness, the values range from 12.7 [mm] to 25.4 [mm] which is the range of wall thickness investigated in [6] . Table 1 and Table 2 summarize the parameter ranges for the planar surface-breaking defect and the planar buried defect equations respectively.

Table 1: Ranges of parameters for planar surface-breaking defect (Minimum, middle, maximum)

δ (mm)	(0.1, 0.2, 0.3)	λ	(0.7, 0.825, 0.95)
η	(0.1, 0.3, 0.5)	ξ	(1, 5.5, 10)

Table 2: Ranges of parameters for planar buried defect (Minimum, middle, maximum)

δ (mm)	(0.1, 0.2, 0.3)	ξ	(1, 5.5, 10)
η	(0.1, 0.3, 0.5)	ψ	(0.1, 0.3, 0.5)
λ	(0.7, 0.825, 0.95)	t (mm)	(12.7, 15.9, 25.4)

RESULTS

The variation of ε_t^{crit} with respect to geometric parameters has been investigated for the case of surface breaking defects when the material properties are constant. This analysis has been carried out for both the equations given in [8] as well as the equations given in [6] . In order to present the difference between the results predicted by [8] and [6] surface plots have been generated visualizing the predicted ε_t^{crit} values for a variation of geometric parameters by fixed material properties. The surface plots in Figure 3 and Figure 4 give an example of the variation of the predicted ε_t^{crit} values according to [6] and [8] . In the surface plots the ranges of the defect geometry parameters have been chosen according to the upper and lower limits specified in [8] . In these plots the lower limit of ξ is set to 1.5. The reason for that was to make both surface plots compatible with each other, since for ξ values lower than 1.5 impractically high ε_t^{crit} values were predicted by the equations of [6] . It can be clearly observed from the surface plots that as expected the tensile strain capacity tends to decrease with increasing defect sizes and there is a non-linear relationship between defect sizes and corresponding tensile strain capacities. The comparison of the predicted ε_t^{crit} values visualized in Figure 3 and Figure 4 shows that the difference between the predictions of [6] and [8] is approximately 6 %.

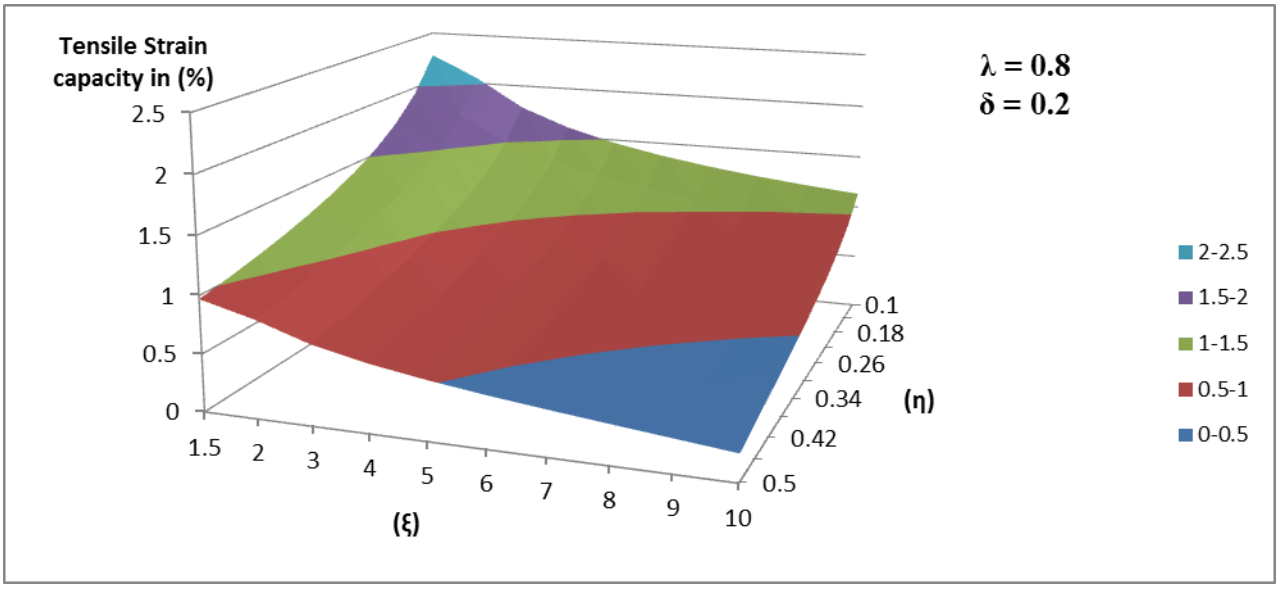

Figure 3: Predicted tensile strain capacities for a variation of defect geometry by constant material properties for surface breaking defects according to CSA Z662-11

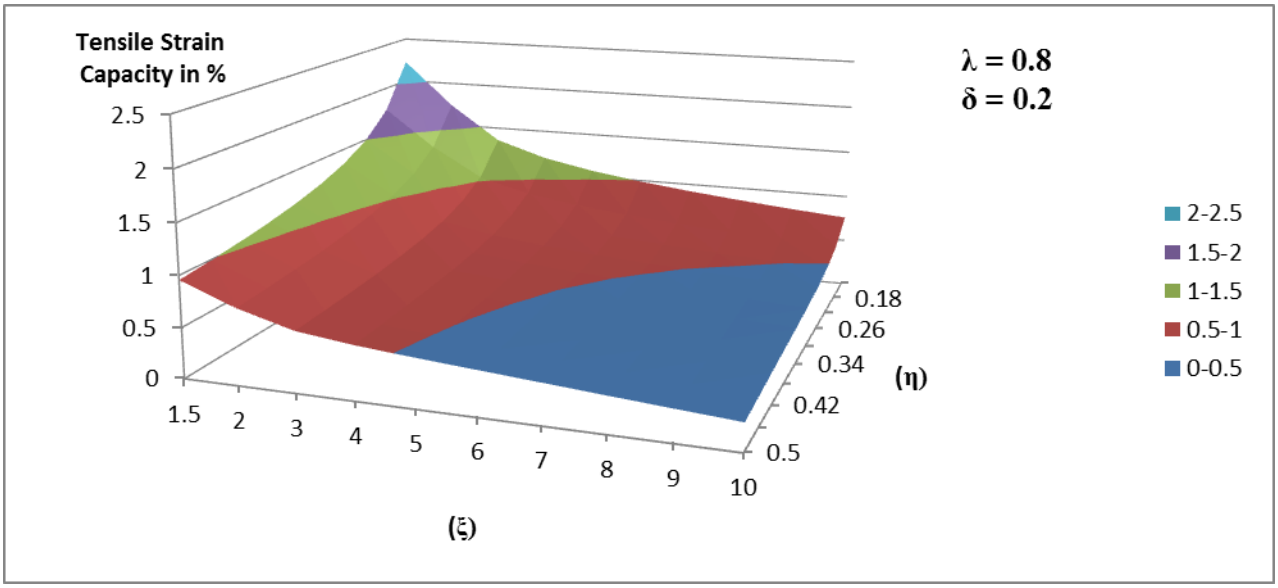

Figure 4: Predicted tensile strain capacities for a variation of material properties by constant defect geometry for surface breaking defects according to [6]

The variation of ε_t^{crit} with respect to material properties for constant geometric parameters has been investigated. The predicted effect of the material toughness (δ) on ε_t^{crit} has been studied in two dimensional plots in Figure 5 and Figure 6. The plots on the left column of Figure 5 show the variation of the relationship between ε_t^{crit} and η with respect to δ for three different values of ξ when λ is fixed at 0.8 which is the intermediate value of the range for λ defined in [8] . Using the plots in the left column of Figure 5, Figure 6 has been generated. In Figure 6 each curve represents the percent change in ε_t^{crit} with respect to the percent change in δ for a particular ξ value. For $\xi = 2,\ 5,\ 8$ the curves were generated at $\eta = 0.5,\ 0.3,\ 0.1$ respectively. The overlapping curves in Figure 6 generated using this method show that for surface breaking defects the variation of ε_t^{crit} with respect to the apparent CTOD toughness δ by fixed geometric parameters is linear and this linear relationship is not affected by the values at which the geometric parameters are fixed.

The predicted effect of the Y/T ratio (λ) on ε_t^{crit} has been studied in two dimensional plots in Figure 5 and Figure 7. These plots confirmed that increasing Y/T values result in lower tensile strain capacities. The plots on the right column of Figure 5 show the variation of the relationship between ε_t^{crit} and η with respect to λ for three different values of ξ when δ is fixed at 0.2 which is the intermediate value of the range for δ defined in [8] . Using the plots in the right column of Figure 5, Figure 7 has been generated. In Figure 7 each curve represents the percent change in ε_t^{crit} with respect to the percent change in λ for a particular ξ value. Again for $\xi = 2,\ 5,\ 8$ the curves have been generated at $\eta = 0.5,\ 0.3,\ 0.1$ respectively. The overlapping curves in Figure 7 generated using this method show that for surface breaking defects the slightly nonlinear relationship between ε_t^{crit} and λ by fixed geometric parameters is independent of the values at which the geometric parameters are fixed.

In order to determine the flaw geometry parameters and material properties having the greatest effect on the predicted ε_t^{crit} value, 3^4 and 3^6 full factorial experimental designs for planar surface breaking defect and buried defect cases have been carried out. ε_t^{crit} has been evaluated at the maximum, minimum and intermediate values of each parameter according to the allowable ranges given in the CSA Z662.11 code which resulted in the evaluation of ε_t^{crit} for 81 different combinations of the parameters for surface breaking defect. The average value of ε_t^{crit} at the maximum, minimum and intermediate value of each parameter has been evaluated using an algorithm which can be customized for different number of geometry and material parameters. The magnitude of the effect of each parameter on the ε_t^{crit} value compared to other parameters has been determined based on the difference between the maximum and minimum values that the average ε_t^{crit} value takes for this parameter. These differences have been listed in Table 3 for the case of surface breaking defect. The visualization of the results in Figure 8 also shows that δ, η and ξ have the greatest effect on ε_t^{crit} among the four parameters for the case of surface breaking defects.

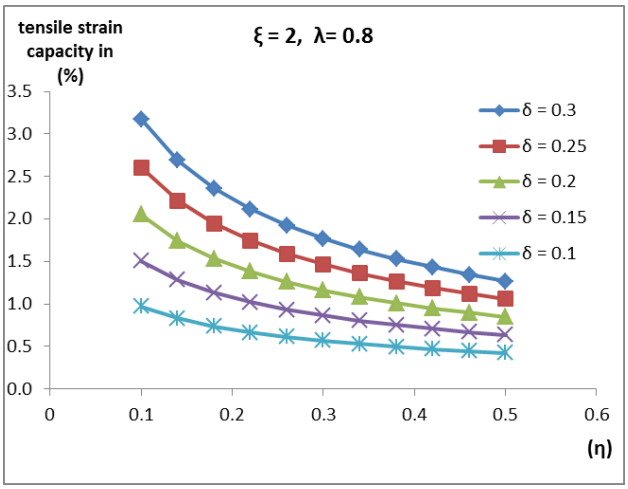

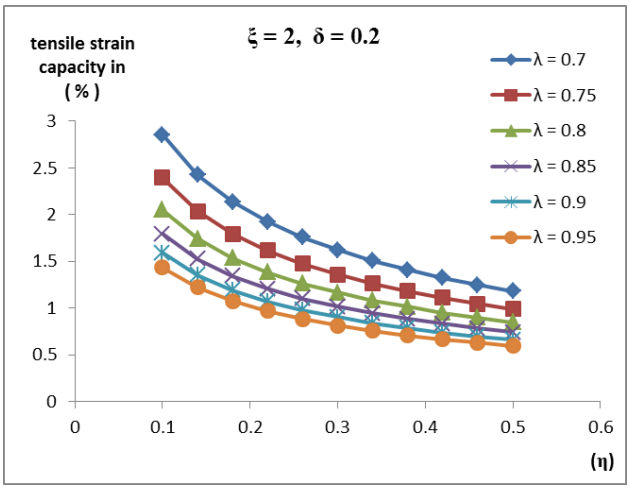

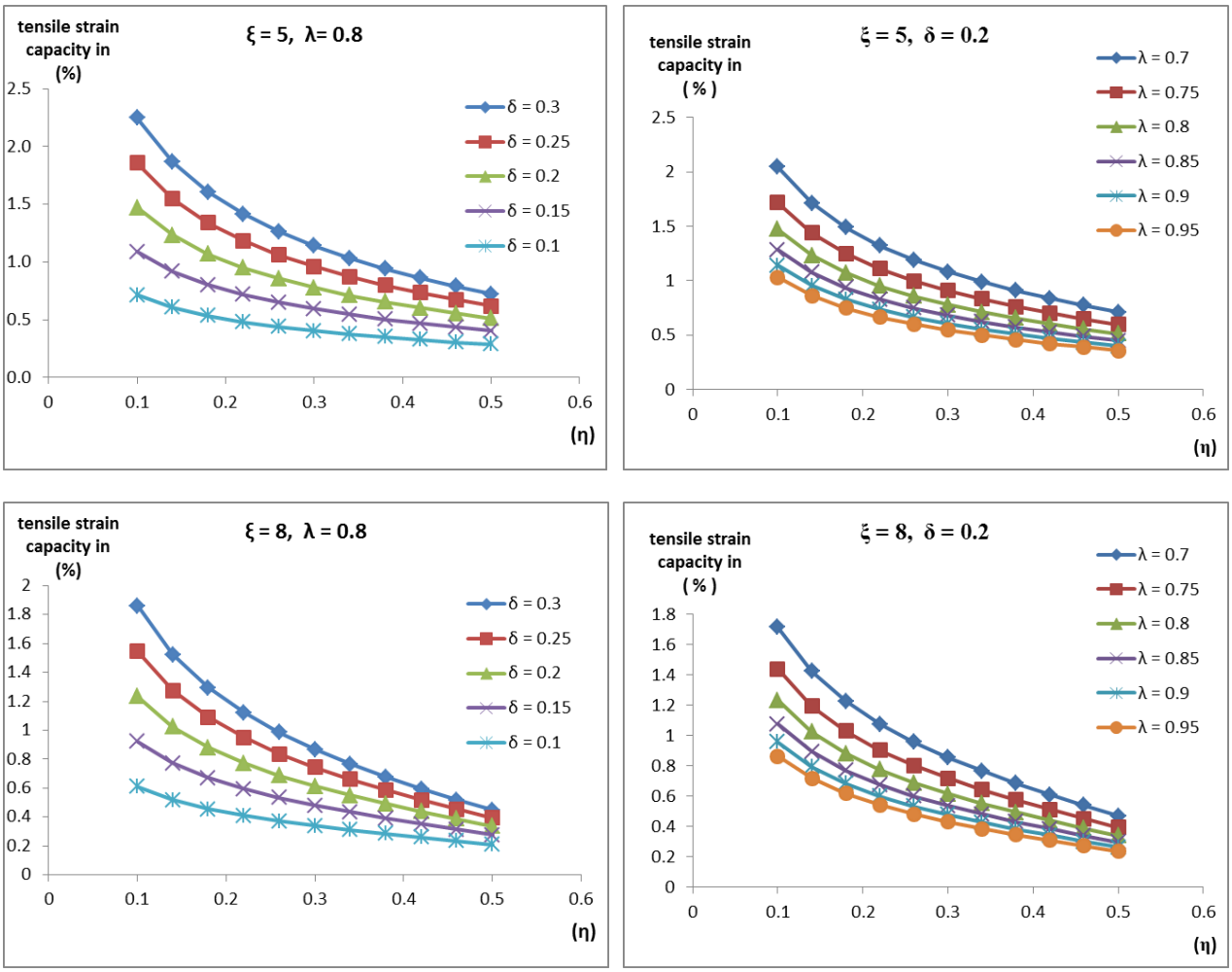

Figure 5: Variation of ε_t^{crit} with material toughness and Y/T ratio according to [8]

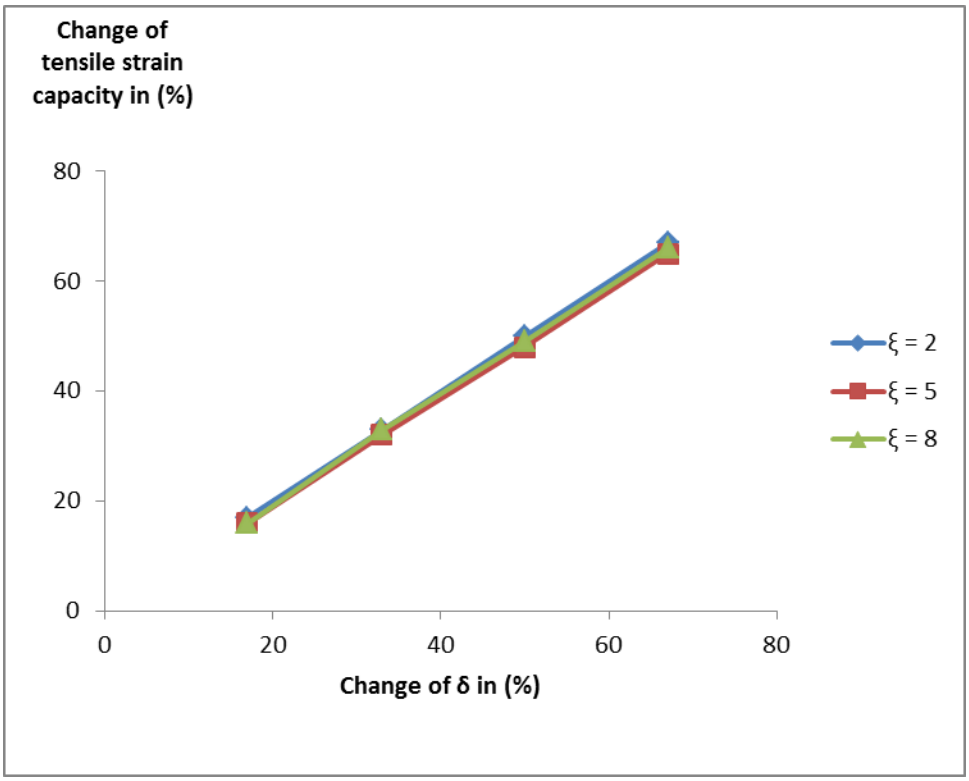

Figure 6: Variation of ε_t^{crit} with respect to δ for $\lambda = 0.8$ according to [8]

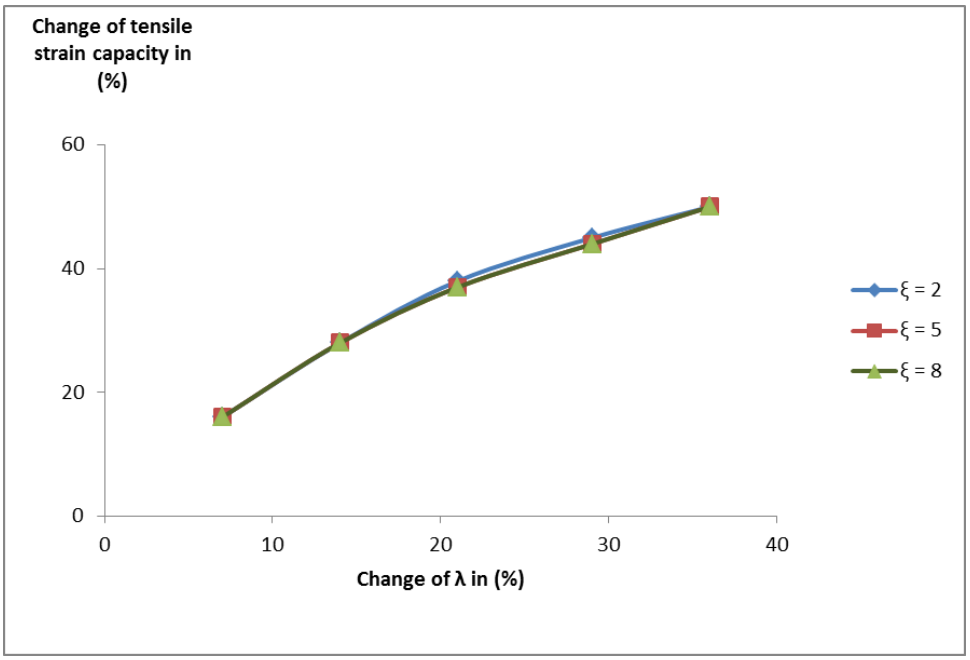

Figure 7: Variation of ε_t^{crit} with respect to λ for $\delta = 0.2$ according to [8]

Table 3: Effect of material and geometric parameters on ε_t^{crit} for surface breaking defect

	Average tensile strain capacity		
	maximum	**minimum**	**difference**
$\boldsymbol{\xi}$	1.849	0.669	1.180
$\boldsymbol{\delta}$	1.729	0.568	1.161
$\boldsymbol{\eta}$	1.745	0.628	1.117
$\boldsymbol{\lambda}$	1.604	0.780	0.824

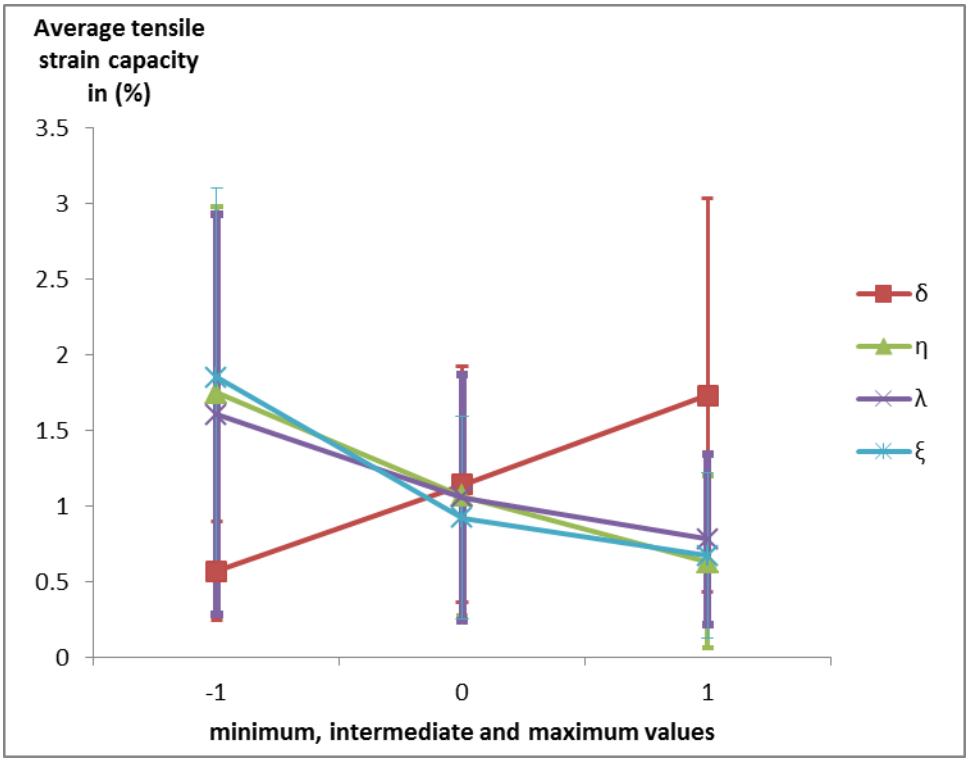

Figure 8: Average value of the tensile strain capacity and standard deviations for maximum, intermediate and minimum value of the defect geometry and material properties for surface breaking defect

Figure 8 shows that the curve of ξ, which demonstrates the greatest variation of ε_t^{crit} over its minimum, intermediate and maximum value has a nonlinear course , while the curves of the other parameters develop rather linearly.

For the case of buried defects the dependence of ε_t^{crit} on defect geometry, pipe thickness and material properties has been studied using a 3^6 full factorial experimental design which lead to the evaluation of ε_t^{crit} for all possible combinations of the maximum, intermediate and minimum values of 6 different parameters. This resulted in ε_t^{crit} being evaluated for 729 different combinations of the minimum, intermediate and maximum values of the defect and material parameters. The average value of ε_t^{crit} at the maximum, minimum and intermediate value of each parameter has been evaluated using an algorithm similar to the one used for the evaluation of ε_t^{crit} for surface defects, which can be customized for different number of geometry and material parameters. The list of differences between the maximum and minimum values of the average ε_t^{crit} for each parameter in Table 4 and the visualization of the results in Figure 9 showed that based on the difference between the maximum and minimum values of the average ε_t^{crit}, η is the parameter having the greatest effect on ε_t^{crit}. The effects of ψ, δ, λ and ξ are in the same order of magnitude whereas t has the least effect on ε_t^{crit} among the 6 parameters for the case of buried defect. Also η, ξ and ψ have a nonlinear course of development while the δ and λ curves demonstrate a very similar course to the case of planar surface breaking defect.

Table 4: Effect of material and geometric parameters on ε_t^{crit} for buried defect

	Average tensile strain capacity		
	maximum	**minimum**	**difference**
$\boldsymbol{\eta}$	6.300	1.053	5.247
$\boldsymbol{\xi}$	4.622	1.850	2.772
$\boldsymbol{\lambda}$	4.162	1.644	2.518
$\boldsymbol{\delta}$	4.064	1.719	2.345
$\boldsymbol{\psi}$	4.388	2.105	2.283
t	3.453	2.464	0.989

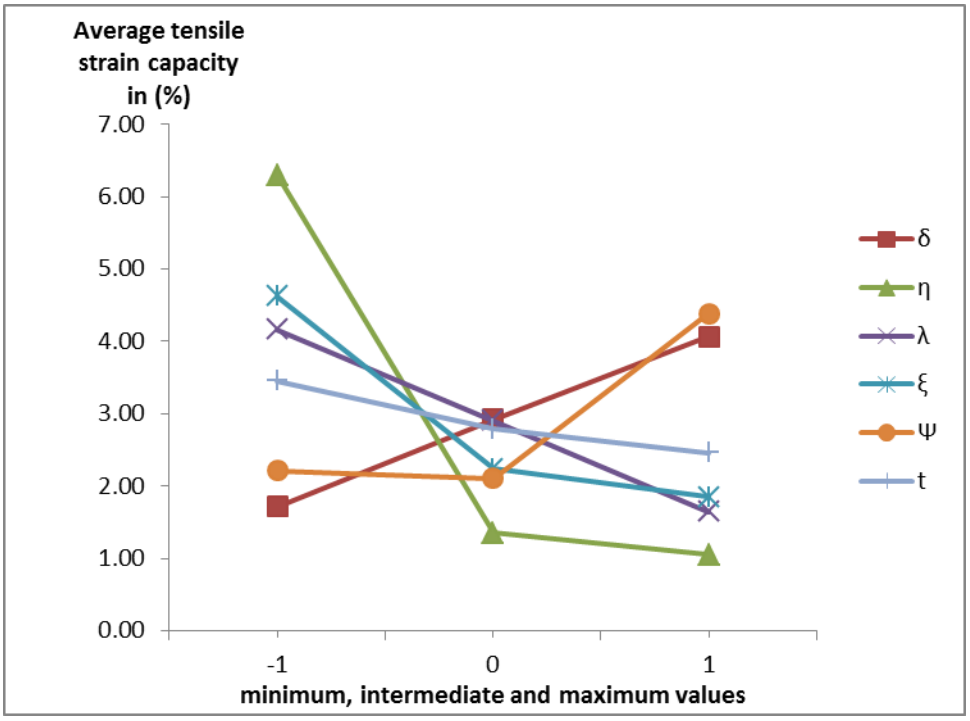

Figure 9: Average value of the tensile strain capacity for maximum, intermediate and minimum value of the defect geometry and material properties for buried defect

DISCUSSION

The equations which have been developed for the prediction of the tensile strain capacity of pipes with flawed girth weld and included in the Canadian standards association code of practice CSA Z662.11 have been studied. For the case of surface breaking defects an example has been demonstrated which visualizes the variation of the predicted ε_t^{crit} values with respect to geometric parameters for fixed material properties in the form of two surface plots according to the equations given in [6] and [8] respectively. The comparison of these surface plots showed that the equations developed in [6] predict approximately 6% lower values for ε_t^{crit}. The decrease in the predicted ε_t^{crit} values can be attributed to the conservative approach adopted in [6] to obtain TSC_0 values from the TSC_p values and to the consideration of the girth weld high-low misalignment in the equations of [6] .

The variation of ε_t^{crit} with respect to material properties for fixed geometric parameters has been studied for surface breaking defects according to [8] . For this purpose the variation of the relationship between ε_t^{crit} and η with respect to the apparent CTOD toughness (δ) has been visualized in the form of the curves in the left column of Figure 5 for 5 different values of δ holding λ fixed at the intermediate value of its range defined in [8] . This procedure has been repeated for 3 different values of ξ. Based on the curves generated for 5 different values of δ a relationship has been constructed between the percent change in δ and the percent change in ε_t^{crit} . The visualization of this relationship in Figure 6 shows that for constant geometric parameters the variation of the percent change in ε_t^{crit} with respect to the percent change in δ is linear and this variation does not depend on the values at which the geometric parameters are fixed.

Similarly the variation of the relationship between ε_t^{crit} and η with respect to the Y/T ratio (λ) has been visualized in form of the curves in the right column of Figure 5 for 5 different values of λ holding δ fixed at the intermediate value of its range defined in [8] for $\xi = 2,\ 5,\ 8$. The visualization of the slightly nonlinear relationship between the percent change in ε_t^{crit} and the percent change in λ which is expected from Eq. (1) is shown in Figure 7 .

3^4 and 3^6 full factorial experimental designs have been applied for the surface defect and buried defect cases respectively. In these experimental designs the minimum, intermediate and maximum values of the parameters were assigned as the lower bound, middle value and upper bound of the ranges defined in CSA Z662.11 code. For those parameters for which no bounded range has been defined in the code, appropriate assumptions have been made. Table 1 and Table 2 define the parameter ranges for both 3^4 and 3^6 full factorial experimental designs. For planar surface breaking defects it was not necessary to make any assumptions about the pipe wall thickness, since this parameter is not explicitly included in the equations (1) and (3). According to Figure 8 the heighest value of the average ε_t^{crit} is about 1.85 % for $\xi = 1$ which is the minimum value for this parameter and the lowest value of the average ε_t^{crit} is about 0.6 % for $\delta = 0.1$ which is the minimum value of δ defined in CSA Z662-11 code. Considering the difference between the maximum and minimum average ε_t^{crit} values of a parameter as a criterion for the effect of this parameter on ε_t^{crit}, it follows from the visualization of the results in Figure 8 that δ, η and ξ have the greatest effect on ε_t^{crit} among the four parameters for the case of surface breaking defects. The significant effect of λ in this case requires further investigation.

For the buried defect case the range of pipe wall thickness has been chosen as (12.7 [mm] , 15.9 [mm], 25.4 [mm]) which is the range investigated in [6] . For the range of ψ, (0.1, 0.3, 0.5) has been chosen as the minimum, intermediate and maximum values which has the same order of magnitude as the range of η. According to Figure 9 the heighest value of the average ε_t^{crit} is about 6.3 % and the lowest value of the average ε_t^{crit} is about 1.05% which occur for the minimum and maximum values of η respectively where the range of η is the same as for the surface breaking defect case. Once again for the buried defects, η was found to have the greatest effect. Again properly measuring the defect height to pipe wall thickness ($2a/t$) is of importance. Looking at pipe thickness (t) independently it was found to have the least difference between the maximum and minimum value of the average ε_t^{crit} and consequently the least effect on the predicted ε_t^{crit} values within the range tested. Over a larger range this may change. Also since it is coupled within many of the other parameters t cannot be ignored. Further investigations could be carried out in order to determine the most appropriate range for ψ. While staying within the boundaries defined in the CSA Z662-11 code the method used could be customised and modified to represent a particular pipe thickness or more specific range of parameters to see their effects. In this way the method could be applied in any pipeline construction project in order to obtain an optimum combination of pipe geometry and material properties in the strain-based design.

REFERENCES

[1] Wang, Y-Y., Cheng W., Horsley D. (2004); "Tensile Strain Limits of Buried Defects in Pipeline Girth Welds" Proceedings of IPC2004, International Pipeline Conference, IPC2004-524

[2] Wang, Y-Y., Chen, Y. (2005); "Reliability Based Strain Design" Gas Research Institute Report 04/0146. Des Plaines, IL.

[3] Wang Y-Y., Cheng, W. (2004); "Guidelines on Tensile Strain Limits" Gas Research Institute Report 04/0030. Des Plaines, IL.

[4] Wang Y-Y., et al (2004); "Tensile Strain Limits of Girth Welds with Surface-Breaking Defects, Part 1 – An Analytical Framework" Proceedings of the 4th International Conference on Pipeline Technology, 235—249

[5] Wang Y-Y., et al (2004); "Tensile Strain Limits of Girth Welds with Surface-Breaking Defects, Part 2 – Experimental Correlation and Validation" Proceedings of the 4th International Conference on Pipeline Technology, 251 – 266

[6] Wang Y-Y.,et al (2011); "Second Generation Models for Strain-Based Design. Contract PR-ABD-1-Project 2. Final Approved Report Prepared for the Design, Materials and Construction Technical Committee of Pipeline Research Council International, (PRCI) Inc.

[7] Montgomery, D.C. (2009); "Design and Analysis of Experiments (7th Edition)"

[8] CSA Z662-11; Oil and gas pipeline systems - Sixth Edition; Update No. 1: January 2012

[9] Wang Y-Y., Liu M. (2010); "Toughness Considerations for Strain Based Design" Proceedings of the 8th International Pipeline Conference, IPC2010-31385